

The Kiselev solution in power-Maxwell electrodynamics

Marina–Aura Dariescu*, Ciprian Dariescu*, Vitalie Lungu*
and Cristian Stelea**

*Faculty of Physics, “Alexandru Ioan Cuza” University of Iasi
Bd. Carol I, No. 11, 700506 Iasi, Romania

**Department of Exact and Natural Sciences,
Institute of Interdisciplinary Research,
“Alexandru Ioan Cuza” University of Iasi,
Bd. Carol I, no. 11, 700506 Iasi, Romania

Abstract

In this work we reconsider the solution describing black holes surrounded by a ‘quintessence’-like fluid. This geometry was introduced by Kiselev in 2003 and its physical source was originally modeled by an anisotropic fluid. We show that the Kiselev geometry is actually an exact solution of the Einstein equations coupled to nonlinear electrodynamics. More specifically, we show that the Kiselev geometry becomes an exact solution in the context of power-Maxwell electrodynamics, using either an electric ansatz or a magnetic one. In both cases the physical source can be modeled by a power-Maxwell Lagrangian, albeit with different powers corresponding to the electric or the magnetic charges. We investigate the timelike and null geodesics in this geometry and show that the solution of the massless Klein-Gordon equation can be expressed by means of the Heun functions, for particular values of the power coefficient q . Finally, we give the proper interpretation of the black-hole thermodynamics in this context. Similarly to the Schwarzschild-de Sitter case, we note the presence of the Schottky peaks in the heat capacity, signaling out the possibility of this thermodynamic black hole system to function as a continuous heat machine.

Keywords: Nonlinear electrodynamics; Klein–Gordon equation; Heun functions;
Quintessence fields

PACS: 04.20.Jb Exact solutions; 02.40.Ky Riemannian geometries; 04.62.+v Quantum fields in curved spacetimes; 02.30. Gp Special functions.

1 Introduction

Astrophysical observations from supernovae (Type Ia) [1, 2], cosmic microwave background radiation (CMBR) [3, 4], Baryon acoustic oscillations (BAO) [5] and the Hubble measurements are suggesting an accelerating expansion of our universe, which may be explained by the presence of dark energy. The defining property of dark energy can be characterized by means of an effective equation of state parameterization of the form $P = w\rho$, where P is the isotropic pressure, while ρ is the energy density. For dark energy fluids one has to restrict $w < -\frac{1}{3}$. For example, a positive cosmological constant Λ corresponds to a dark energy model for which $w = -1$ (see the review [6] and references therein).

One of the candidates for dark energy is the quintessence [7, 8] (see also [9] and the references within), which can be seen as a canonical scalar field coupled to gravity whose potential is decreasing as the field increases. A slowly varying scalar field ϕ with an appropriate scalar potential $V(\phi)$ can lead to the accelerated expansion of the Universe [10]. At the cosmological level, the role of the scalar field has also been investigated in [11], where the Einstein–Klein–Gordon equations for Friedmann–Robertson–Walker geometries were analyzed. However, it has been proved that the origin of quintessence at the cosmological and galaxy scales could be significantly different, in the sense that the quintessence state parameter w can have different values [12].

Almost twenty years ago, a spherically-symmetric static solution of Einstein equations, describing black holes surrounded by ‘quintessence’-like fluids has been found by Kiselev [13]. The Kiselev geometry is sourced by an anisotropic fluid [14], [15] that behaves like a kind of dark energy since its equation of state is $p_r = -\rho$, with $p_r \neq p_t$, where p_r is the radial pressure, while p_t denotes the tangential pressures p_θ and p_φ . The isotropic pressure is $P = \frac{1}{3}(p_r + 2p_t) = w\rho$, where w is the Kiselev quintessence parameter. Therefore, in order to cause the accelerated expansion of the universe, the equation of state parameter w should be in the range $w \in [-1, -1/3]$. In the particular case $w = -2/3$, one gets in the metric function an additional linear contribution, $-kr$. The parameter k , which is the Kiselev quintessence charge can lead to a metric that was previously used in modified Newtonian dynamics (MOND) [16], and various other modifications of General Relativity [17], [18] (see also [19] and [20]).

In this paper we propose a physical source for the Kiselev geometry in the context of nonlinear electrodynamics. This class of theories has a long history, as they were introduced initially in order to cure the infinite electric field and the infinite self-energy for point-like charged particles. The first model was introduced by Born and Infeld in 1934 [21] and it was soon realized that nonlinear electrodynamics theories could act as effective classical

modifications from QED [22]. Nowadays, the nonlinear electrodynamics theories are an active area of research and they provided us with various interesting black hole solutions in four and higher dimensions (for a review and more references see [23] and [24]). Generically, the nonlinear Lagrangian is constructed from the two quadratic electromagnetic invariants $F_{\mu\nu}F^{\mu\nu}$ and $F_{\mu\nu}\star F^{\mu\nu}$, where $\star F^{\mu\nu}$ is the dual of $F_{\mu\nu}$ [25] (see also [26]). Here we will focus on a simpler Lagrangian $L = L(F)$ that depends only the first electromagnetic invariant, $F = F_{\mu\nu}F^{\mu\nu}$. From the least action principle we then obtain the following field equation for the nonlinear electromagnetic field:

$$\partial_\mu (\sqrt{-g} L_F F^{\mu\nu}) = 0, \quad (1)$$

where L_F is the derivative of the function L with respect to the variable F .

In our work we will consider the so-called power-Maxwell model, for which the electromagnetic Lagrangian is defined as $-\alpha(F_{\mu\nu}F^{\mu\nu})^q$, where α is a coupling constant that has to be introduced in order to have a positive energy density of the nonlinear Maxwell field [27], [28]. In spaces with d dimensions it turns out that the power-Maxwell electrodynamics can still enjoy conformal invariance if the power coefficient q in the Lagrangian is equal to $\frac{d}{4}$ [29]. For more properties of the solutions of the power-Maxwell theory in various theories and various dimensions see also [30] - [35].

Within this nonlinear electrodynamics theory, we show that the Kiselev solution becomes an exact solution of the Einstein-power-Maxwell equations (with or without cosmological constant) using either an ansatz involving electric charges and fields, or a magnetic monopole ansatz¹. In both cases we show how one can relate the Kiselev quintessence parameters w and k to the corresponding electric charge Q_e or the magnetic charge Q_m and the power coefficient q appearing in the power-Maxwell Lagrangian. We then describe some of the properties of these solutions: we study the motion of particles around these black holes, noting that light will travel on the null-geodesics defined by an ‘‘effective geometry’’, instead of the null geodesics of the background geometry [37], [23], [38].

The motion of particles moving around different types of black holes surrounded by ‘quintessence’ has been extensively studied in recent years. In this respect, for the Schwarzschild black hole surrounded by ‘quintessence’, the null and timelike geodesics have been investigated by many authors, see for instance [39]-[43]. In the present paper, we are discussing the effective potential and the timelike geodesics for particles moving around the black hole described by Kiselev’s solution as an exact solution of the power-Maxwell nonlinear electrodynamics. By comparing the results with those for the usual Schwarzschild black hole, one can point out the effects of the nonlinear electromagnetic fields.

¹An exact solution involving a regular Bardeen black hole with quintessence was previously found in [36].

The structure of this paper is as follows: in the next section we review the properties of the Kiselev solution that describes a black hole surrounded by a quintessence-like anisotropic fluid. In section 3 we introduce the power-Maxwell theory and show that the Kiselev solution becomes an exact solution in this theory. In section 4 we discuss the geodesic motion for timelike and null cases. In section 5 we show that for particular power coefficients the Klein-Gordon equation can be solved analytically and its solutions can be expressed in terms of the confluent Heun functions and we discuss the eikonal approximation. In section 6 we approach the thermodynamic properties of the Kiselev black holes. In particular, we point out the presence of the Schottky peaks in the heat capacity [44], [45], [46] which hints to the possibility of interpreting the Kiselev black hole as a continuous heat machine. Section 7 is dedicated to conclusions and avenues for further work.

2 The Kiselev geometry

The Kiselev geometry is described by the following static four-dimensional line-element [13]:

$$ds^2 = -g_{00}dt^2 + \frac{dr^2}{g_{00}} + r^2(d\theta^2 + \sin^2\theta d\varphi^2), \quad (2)$$

where

$$g_{00} = 1 - \frac{2M}{r} - \frac{k}{r^{3w+1}}. \quad (3)$$

Here w is the equation of state parameter and k is a positive quintessence parameter, which is related to the fluid quintessence energy density ρ :

$$\rho = -\frac{3kw}{r^{3(w+1)}},$$

while components of the anisotropic pressures can be written as $p_r = -\rho$ and the tangential pressures are given by:

$$p_\theta = p_\varphi = -\frac{3(3w+1)kw}{2r^{3(w+1)}}. \quad (4)$$

In order to have an accelerated expansion, the equation of state parameter w should belong to the interval $w \in [-1, -1/3]$.

The horizons of this geometry will correspond to solutions of the equation $g_{00} = 0$. As it can be noticed in Figure 1, for fixed values of M and k , one may have, besides the black hole's horizon r_b , situated just after $2M$, an additional (outer) quintessence horizon, r_q . The two horizons are given by the intersection between the $f(r) = g_{00}$ sheet and the $r = 0$ plane. Once w is decreasing to the limiting value $w \rightarrow -1$, the quintessence horizon comes closer to the black hole's horizon. In the opposite case where w is increasing to $w \rightarrow -1/3$, the

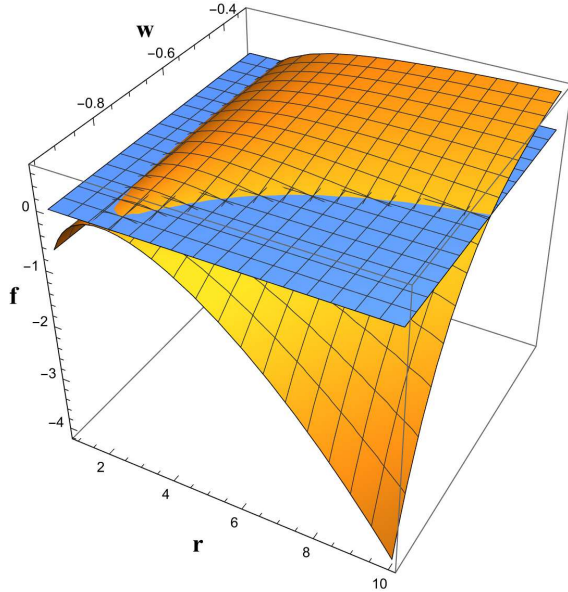


Figure 1: The metric function $f(r) = g_{00}$ given in (3), for $w \in [-1/3, -1]$ with $M = 0.8$ and $k = 0.2$. The blue plane corresponds to $g_{00} = 0$.

quintessence horizon moves to bigger values of the radial coordinate. For $w = -1/3$, we have a static black hole surrounded by a spherically symmetric cloud of strings, with

$$g_{00} = 1 - k - \frac{2M}{r}, \quad (5)$$

and the unique horizon

$$r_b = \frac{2M}{1 - k}. \quad (6)$$

This spacetime is still singular as it contains conical singularities. There is no quintessence horizon, the effect of the quintessence fluid being encoded only in the constant k , which is responsible for the deficit or the excess of solid angle.

For the limiting value $w = -1$, one recovers the Schwarzschild-de Sitter geometry, with

$$g_{00} = 1 - \frac{2M}{r} - kr^2.$$

In this case, three real roots of the corresponding cubic equation, among which two are positive, are obtained for the relation between the parameters $27kM^2 < 1$. Otherwise, one has one real root and two complex conjugated roots.

The physically important case corresponding to $w = -2/3$ is particularly simple, since one has a linear contribution in the metric function, which becomes:

$$g_{00} = 1 - \frac{2M}{r} - kr. \quad (7)$$

The two horizons, solution of the equation $g_{00} = 0$, are obtained for $8kM < 1$ and they are given by:

$$r_{\pm} = \frac{1}{2k} \left[1 \pm \sqrt{1 - 8kM} \right]. \quad (8)$$

For $8kM \ll 1$, these have the expressions

$$r_- = r_b \approx 2M(1 + 2kM), \quad r_+ = r_q \approx \frac{1 - 2kM}{k}.$$

However, note that if $M = 0$, *i.e.* in absence of the black hole horizon, while the geometry still has a quintessence horizon, located at r_c , there is a naked curvature singularity in origin unless $w = -1$ and $w = -\frac{1}{3}$. In this case the quintessence horizon plays the role of a cosmological horizon, similar to the de Sitter case.

3 The Kiselev solution in power-Maxwell electrodynamics

One interesting class of nonlinear electromagnetic sources is the power-Maxwell theory. The full action in this case is given by [27], [28]:

$$I = -\frac{1}{16\pi G} \int_{\mathcal{M}} d^4x \sqrt{-g} (R - \alpha F^q) - \frac{1}{8\pi G} \int_{\partial\mathcal{M}} d^3x \sqrt{-\gamma} K, \quad (9)$$

where we denoted $F = F_{\mu\nu}F^{\mu\nu}$ and K is the usual Gibbons-Hawking boundary term, defined on the spacetime boundary $\partial\mathcal{M}$, on which the induced metric is denoted by γ_{ab} .

The field equations derived from this action can be written in the form:

$$G_{\mu\nu} = T_{\mu\nu} \quad (10)$$

$$\partial_{\mu} (\sqrt{-g} F^{\mu\nu} F^{q-1}) = 0, \quad (11)$$

where the stress-energy tensor of the electromagnetic field is defined as:

$$T_{\mu\nu} = 2\alpha \left[q F_{\mu\rho} F_{\nu}^{\rho} F^{q-1} - \frac{1}{4} g_{\mu\nu} F^q \right]. \quad (12)$$

We are looking for a spherically-symmetric geometry of the Kiselev form:

$$ds^2 = -f(r)dt^2 + \frac{dr^2}{f(r)} + r^2(d\theta^2 + \sin^2\theta d\varphi^2) \quad (13)$$

where

$$f(r) = 1 - \frac{2M}{r} - kr^p. \quad (14)$$

Here k is a positive parameter, which can be related to the original quintessence parameter in Kiselev's solution, while $p = -(3w + 1)$ is now a positive parameter. If $w \in [-1, -\frac{1}{3}]$ then $0 \leq p \leq 2$, although in the general solution one can keep p general.

3.1 The electric ansatz

If the geometry is sourced by nonlinear electric fields we shall use the following ansatz for the electromagnetic potential:

$$A_\mu = (\chi(r), 0, 0, 0), \quad (15)$$

from which one constructs the Maxwell tensor $F_{\mu\nu} = \partial_\mu A_\nu - \partial_\nu A_\mu$. A quick computation reveals that the electromagnetic invariant takes the form $F = -2 \left(\frac{d\chi}{dr} \right)^2 < 0$, which allows us to pick $\alpha = (-1)^{(-q)}$ in the action, in order to have a positive-definite energy of the electromagnetic field for $q < 0$. More specifically, if one computes the components of the electromagnetic stress-energy tensor (12), then the energy density of the electromagnetic field is:

$$\rho = -T_t^t = \frac{\alpha F^q (1 - 2q)}{2}. \quad (16)$$

One can see that one can choose $\alpha = (-1)^{-q}$ if $q < \frac{1}{2}$ and $\alpha = -(-1)^{-q}$ if $q > \frac{1}{2}$ if the energy density ρ is to be positive-definite. In our case, for the Kiselev solution with quintessence we will see below that the power parameter q can take only negative values, such that $\alpha = (-1)^{-q}$ is the appropriate choice.

One can now solve directly the equation of motion for the nonlinear electromagnetic field in (11) and one obtains:

$$\chi(r) = C_1 + C_2 r^{p+1}, \quad (17)$$

where C_1 and C_2 are constants of integration.

Solving now the Einstein equations in (11) one can further find that the value of the power coefficient q must be restricted in terms of the parameter p as² :

$$q = \frac{p-2}{2p}, \quad (18)$$

while the quintessence parameter k in (14) can be written as:

$$k = \frac{2^{\frac{1}{2} - \frac{2}{p}} C_2^{1 - \frac{2}{p}} (p+1)^{-\frac{2}{p}}}{p}. \quad (19)$$

The constant C_2 can be directly related to the electric charge Q_e of this black hole solution. The electric charge can be computed using the formula:

$$Q_e = -\frac{\alpha}{4\pi} \int_{S^2} (F)^{q-1} \star F = 2^{-\frac{p+2}{2p}} C_2^{-\frac{2}{p}} (p+1)^{-\frac{2}{p}}, \quad (20)$$

²Note that for $0 \leq p \leq 2$ the power $q < 0$ such that $\alpha = (-1)^{-q}$ is the right choice.

where $\star F_{\mu\nu} = \frac{1}{2}\sqrt{-g}\epsilon_{\mu\nu\alpha\beta}F^{\alpha\beta}$ is the dual of the Maxwell tensor $F_{\mu\nu}$, with $\epsilon_{\mu\nu\alpha\beta}$ being the Kronecker symbol, while S^2 is a 2-sphere containing the black hole horizon.

Combining now (19) and (20) one can re-express the constant C_2 in (17) as

$$C_2 = \frac{Q_e^{-\frac{p}{2}}}{2^{\frac{p+2}{4}}(p+1)} \quad (21)$$

Finally, the parameter k appearing in the metric (14) can be expressed in terms of the electric charge Q_e in the particularly simple form:

$$k = \frac{2^{\frac{2-p}{4}}Q_e^{\frac{2-p}{2}}}{p(p+1)}. \quad (22)$$

Note that the obtained solution is valid for every value of the parameter p and it can be easily modified to accommodate the presence of a cosmological constant Λ in (9) and (14).

3.1.1 The energy conditions using the electric ansatz

One can now easily check the energy conditions satisfied by the nonlinear electromagnetic field in our solution. Recall that in the original Kiselev solution with quintessence the parameter $p \in [0, 2]$ such that $q \leq 0$. More specifically, if one denotes the effective tangential pressures in the electromagnetic stress-energy tensor (12) by:

$$p_\theta = p_\varphi = -p_0, \quad (23)$$

then one can express the energy density ρ and the radial pressure p_r as:

$$\rho = -p_r = p_0(1 - 2q), \quad (24)$$

where we defined

$$p_0 = \frac{\left[2\left(\frac{dx}{dr}\right)^2\right]^q}{2} > 0. \quad (25)$$

It is now easy to check that the Weak Energy Condition (WEC), which requires $\rho \geq 0$ and $\rho + p_r \geq 0$ and $\rho + p_t \geq 0$ is satisfied for $q \leq 0$. Similarly, the Dominant Energy condition (DEC), which requires that $\rho \geq 0$ and $-\rho \leq p_r \leq \rho$ and $-\rho \leq p_t \leq \rho$ is satisfied as well. However, the Strong Energy Condition (SEC) is not satisfied since $\rho + p_r + 2p_t < 0$ in our case.

3.2 The magnetic ansatz

It is interesting to note that the same geometry defined by (14) can also be sourced by using a magnetic monopole ansatz for the electromagnetic potential. More specifically, we shall choose:

$$A_\mu = (0, 0, 0, Q_m(1 - \cos \theta)), \quad (26)$$

where Q_m is a constant that can be shown to be equal to the magnetic charge in our solution. Indeed, in this case the magnetic monopole charge is defined by the equation:

$$Q_m = \frac{1}{4\pi} \int_{S^2} F, \quad (27)$$

where $F = Q_m \sin \theta d\theta \wedge d\varphi$ denotes here the electromagnetic 2-form, not to be confused with the electromagnetic invariant $F = F_{\mu\nu} F^{\mu\nu}$ that we used in the action (9). In fact, it can be shown by direct computation that this invariant takes now the particularly simple form $F = \frac{2Q_m^2}{r^4} \geq 0$. Since this invariant is always positive, one can simply take $\alpha = 1$ in the action (9) since we are guaranteed that the energy density of the electromagnetic field is now positive for any power coefficient q . Moreover, with this magnetic ansatz the nonlinear Maxwell equations in (11) are satisfied as well.

Solving now the Einstein equations in (11) one finds that they are identically satisfied if one takes the following parameters:

$$q = \frac{2-p}{4} \quad (28)$$

in the action (9) and

$$k = \frac{(2Q_m^2)^{\frac{2-p}{4}}}{2(p+1)} \quad (29)$$

in the metric (14). This completes our solution using the magnetic ansatz. Note that if $p \in [0, 2]$, then the power coefficient q belongs to the interval $0 \leq q \leq \frac{1}{2}$.

3.2.1 The energy conditions using the magnetic ansatz

One can now discuss the energy conditions satisfied by our nonlinear electromagnetic field using the magnetic ansatz. If one considers the diagonal components of the corresponding stress-energy tensor (12):

$$T^\mu_\nu = \text{diag}(-\rho, p_r, p_\theta, p_\varphi) \quad (30)$$

then one finds $\rho = -p_r = \frac{2p_0}{p}$ and $p_\theta = p_\varphi = -p_0$, where we defined p_0 by:

$$p_0 = \frac{p \left(\frac{2Q_m^2}{r^4} \right)^q}{4}. \quad (31)$$

Note that for the Kiselev with quintessence geometry one has $0 \leq p \leq 2$ and therefore the quantity p_0 is positive.

One can now easily check that the weak energy condition (WEC) and the dominant energy condition (DEC) are both satisfied for $0 \leq p \leq 2$, while the strong energy condition (SEC) is violated since $\rho + p_r + p_\theta + p_\varphi = -2p_0 < 0$, just as in the electric case.

3.3 The location of the horizons

We shall now describe some of the properties of the solutions found in the power-Maxwell nonlinear electrodynamics. First, let us discuss the location of the horizons in the geometry defined by (14). Recall that in our case $p \in [0, 2]$ and $k > 0$.

The horizons will correspond to solutions of the equation $f(r) = 0$. Even if, for general powers p , one cannot solve this equation analytically, it is still possible to draw some general conclusions regarding the location of the horizons. For this, let us define a new variable $u = \frac{1}{r}$ such that $f(u) = 1 - 2Mu - ku^{-p}$. Then the solutions of the equation $f(u) = 0$ will correspond to the intersection points of the line $y_1 = 1 - 2Mu$ with the curve $y_2 = ku^{-p}$ (see Figure 2). One can see that depending on the values taken by M , p and Q one can have at most two horizons: a black hole horizon located at r_b and one horizon (the quintessence horizon in the original Kiselev solution) located at $r_c > r_b$. This second horizon plays the role of an effective cosmological horizon and the static patch of the Kiselev geometry is now restricted to values of the radial coordinate r in between these two horizons. Outside the ‘cosmological’ horizon r_c the radial coordinate becomes timelike and the temporal coordinate becomes spacelike, just as it happens in the Schwarzschild-de Sitter geometry. There is however a marked difference to the Schwarzschild-de Sitter case, since in absence of the black hole horizon there is a naked singularity in the bulk, unless $p = 2$ (which corresponds to an effective de Sitter geometry) or $p = 0$, which corresponds to a conical singularity.

As one increases the black hole mass parameter, M , the black hole horizon r_b increases while the cosmological horizon r_c shrinks. For fixed Q and p values there is a maximum value of the mass parameter M such that the two curves y_1 and y_2 have only one point of intersection, located at

$$r_0 = \frac{2(p+1)M}{p}. \quad (32)$$

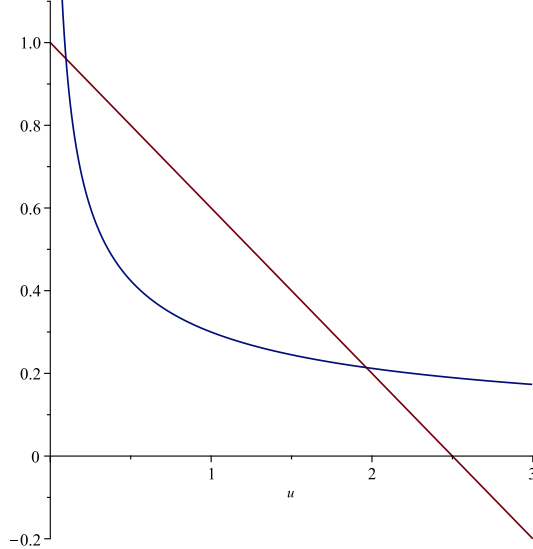


Figure 2: The intersection of the line described by y_1 for $M = 0.2$ and the curve y_2 for $k = 0.3$ and $p = 0.5$.

This situation corresponds to the extremal case, similar to the Nariai solution in the Schwarzschild-de Sitter case. The maximum value of the mass parameter can be expressed as:

$$M_{max} = \frac{1}{2}p(p+1)^{\frac{p-1}{2-p}}k^{\frac{1}{2-p}}, \quad (33)$$

where k is given by (19) in the electric case and (29) in the magnetic solution.

If the mass parameter is increased beyond this value the spacetime becomes singular, as it contains now a naked singularity. The lesson to be learnt is that the black hole horizon r_b can only have values in between 0 and r_0 , otherwise the spacetime geometry is singular.

4 Particle orbits in the power-Maxwell Kiselev background

In this section we shall briefly discuss the trajectories of particles in the Kiselev geometry as parameterized in (14). These trajectories have been previously discussed in literature in the timelike and the null case [39] - [41]. Since our solution is an exact solution of a nonlinear electrodynamics theory, one should note that photons will follow the null geodesics of an “effective” geometry instead of the null geodesics of the Kiselev background [37].

4.1 Timelike trajectories

The trajectory of a massive test particle with mass μ and charge e can be determined by using the Lorentz-force equation. In this case it reads:

$$\frac{d^2x^\mu}{d\tau^2} + \Gamma_{\alpha\beta}^\mu \frac{dx^\alpha}{d\tau} \frac{dx^\beta}{d\tau} = -\frac{e}{\mu} F_\sigma^\mu \frac{dx^\sigma}{d\tau}, \quad (34)$$

where τ is the proper time along its trajectory. The proper time τ is defined by using the equation:

$$-d\tau^2 = -f(r)dt^2 + \frac{dr^2}{f(r)} + r^2(d\theta^2 + \sin^2\theta d\varphi^2), \quad (35)$$

For a particle which is freely falling in the equatorial plane ($\theta = \pi/2$), the conserved energy E and angular momentum L are given by

$$E = f(r)\dot{t}, \quad L = r^2\dot{\varphi}, \quad (36)$$

where *dot* means the derivative with respect to τ . Using the two conserved quantities E and L along the trajectory, one can re-express the equation (35) as describing the motion of particle in an effective potential:

$$\frac{1}{2}\dot{r}^2 + \frac{1}{2}f(r)\left[1 + \frac{L^2}{r^2}\right] - \frac{E^2}{2} = 0, \quad (37)$$

pointing out the effective potential

$$V_{eff} = \frac{1}{2}f(r)\left[1 + \frac{L^2}{r^2}\right] = \frac{1}{2}\left[1 - \frac{2M}{r} - kr^p\right]\left[1 + \frac{L^2}{r^2}\right], \quad (38)$$

that is felt by a charged test particle.

The situation is simpler for a particle with zero angular momentum $L = 0$ for which the relations (37) and (38) turn into

$$\dot{r}^2 = E^2 - f(r), \quad (39)$$

and

$$V_{eff} = \frac{1}{2}\left(1 - \frac{2M}{r} - kr^p\right) \quad (40)$$

and the ‘effective’ force acting on the particle has the expression

$$F = -V'_{eff} = -\frac{1}{r^2}[2M - pkr^{p-3}].$$

This effective force is attractive for $p \leq 0$, as in the Schwarzschild case, and it can have both attractive and repulsive contributions for $p > 0$. The maxima of the effective potential are

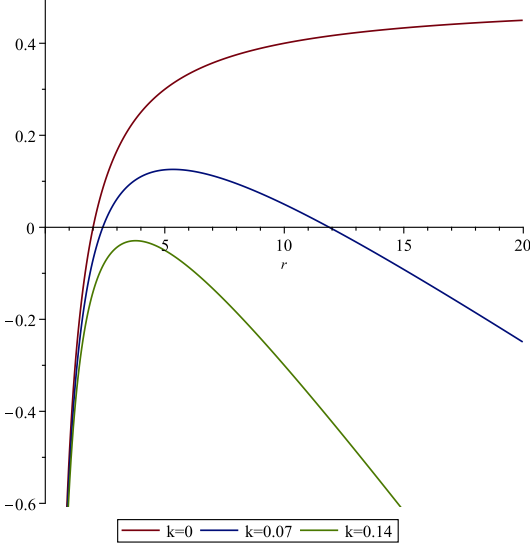


Figure 3: The effective potential given by (42) with $M = 1$ for the Schwarzschild black hole, *i.e.* $k = 0$, and for the power-Maxwell black hole with $k = 0.07$, respectively for $k = 0.14$.

found by solving $F = 0$ and one finds the root $r_0 = \left(\frac{2M}{kp}\right)^{\frac{1}{p+1}}$. The maximum value of the effective potential is:

$$V_{eff}^{max} = \frac{1}{2} \left[1 - \frac{2M}{r_0} \frac{p+1}{p} \right]. \quad (41)$$

As an example, in Figure 3, we have represented the effective potential (38) for $p = 1$, *i.e.*

$$V_{eff} = \frac{1}{2} \left(1 - \frac{2M}{r} - kr \right), \quad (42)$$

for different values of the parameter k . The usual Schwarzschild black hole, *i.e.* $k = 0$, is represented by the red line, while the other solid lines correspond to the black hole in the nonlinear electrodynamics for nonzero values of k . One may notice that, for $k < 1/(8M)$, the potential has a positive maximum, $V_{max} = 1 - \sqrt{8kM}$, in $r_0 = \sqrt{2M/k}$, and therefore there are two solutions of the equation $V_{eff} = 0$, given by the intersection of the solid curve with the horizontal axis. Once k is increasing, the curve is approaching the horizontal axis. For $8kM > 1$, the maximum of the potential moves below the horizontal axis, pointing out the formation of a naked singularity.

In order to have a circular orbit, with $r = R_c$, one has to impose the conditions $\dot{r} = 0$ and $\ddot{r} = 0$, *i.e.*

$$V_{eff}(r = R_c) = E^2, \quad V'_{eff}(r = R_c) = 0. \quad (43)$$

For an arbitrary parameter p , the second equation in (43) leads to the radius

$$R_c = r_0 = \left(\frac{2M}{kp} \right)^{\frac{1}{p+1}} \quad (44)$$

and one may notice that for $p < 0$ there are no circular orbits. If $p = 2$, the circular orbit has the radius

$$R_c = \left(\frac{M}{k} \right)^{1/3}$$

and the corresponding effective potential in $r = R_c$ reads

$$V_{eff} = 1 - 3(kM^2)^{1/3}.$$

Since $V''_{eff} = -6k < 0$, the circular orbit is unstable.

In the physically important case $p = 1$, the circular radius is

$$R_c = \sqrt{\frac{2M}{k}}, \quad (45)$$

and the effective potential gets a maximum value

$$V_{eff}(r = R_c) = 1 - \sqrt{8kM} = V_{max}. \quad (46)$$

Thus, the particle with $E^2 = 1 - \sqrt{8kM}$ has an unstable circular orbit [39], [43].

4.2 Null trajectories

Finally, let us briefly turn our attention to the null geodesics of the metric (13). For a detailed study of the null geodesics and circular orbits for the Kiselev black hole see [39], [41].

For the line element (13), with the metric (14) and the conserved quantities (36), in the equatorial plane (for $\theta = \frac{\pi}{2}$) one obtains the following relation

$$\dot{r}^2 = E^2 - f(r) \frac{L^2}{r^2} \quad (47)$$

pointing out the effective potential

$$V_{eff}(r) = f(r) \frac{L^2}{2r^2} = \left(1 - \frac{2M}{r} - kr^p \right) \frac{L^2}{2r^2}. \quad (48)$$

In order to find the null circular orbits, we impose the conditions (43) which lead to the radius values r_0 that are solutions of the equation:

$$1 - \frac{2M}{r_0} - \frac{2E^2 r_0^2}{L^2} = \frac{1}{p-2} \left(\frac{6M}{r_0} - 2 \right). \quad (49)$$

For example, if $p = 1$ then one obtains:

$$r_0 = \frac{1 \mp \sqrt{1 - 6kM}}{k} \quad (50)$$

and the following relations between the energy and the angular momentum:

$$\frac{E^2}{L^2} = \frac{1 - 9kM \pm (1 - 6kM)^{3/2}}{54M^2} = \frac{r_0 - 2M - kr_0^3}{r_0^3}. \quad (51)$$

For $6kM \ll 1$, one of the circular radius is close to the last Schwarzschild circular orbit $r_0 = 3M$, while the other one, $r \approx (2 - 3kM)/k$, is not physical since it leads to a negative value for the right hand side of the relation (51).

4.3 Photon orbits for the black hole in the power-Maxwell electrodynamics

Even if we considered above the null geodesics, one should note that photons behave differently in the context of a nonlinear electrodynamics as compared to the standard linear theory of Maxwell electrodynamics [37], [23], [38].

More precisely, photons will follow the null geodesics of an effective geometry given by [37]:

$$g_{eff}^{\mu\nu} = L_F g^{\mu\nu} - 4L_{FF} F_\alpha^\mu F^{\alpha\nu}, \quad (52)$$

where L_{FF} is now the second derivative of the power-law Lagrangian with respect to the electromagnetic invariant $F = F_{\mu\nu} F^{\mu\nu}$. In our case $L = -\alpha F^q$ such that $L_F = -\alpha q F^{q-1}$ and $L_{FF} = -\alpha q(q-1) F^{q-2}$.

Since we are considering the null orbits of the effective geometry, it will suffice to take into account a conformally rescaled effective geometry of the form bellow that will lead to the same null geodesics:

$$g_{\mu\nu}^{resc} = g_{\mu\nu} - \frac{4(q-1)}{F} F_{\mu\alpha} F_\nu^\alpha. \quad (53)$$

It is now easy to check that in this case the null geodesics of the rescaled effective geometry satisfy the following equation in the equatorial plane $\theta = \frac{\pi}{2}$:

$$-f(r)\dot{t}^2 + \frac{\dot{r}^2}{f(r)} - \frac{p}{2}r^2\dot{\phi}^2 = 0, \quad (54)$$

if one uses the electric ansatz for the metric. Formally, taking now into account the conserved quantities (36) one can readily identify the modified effective potential³

$$V_{eff}(r) = -\frac{1}{p} \left(1 - \frac{2M}{r} - kr^p \right) \frac{L^2}{r^2}. \quad (55)$$

³Note that the conserved angular momentum becomes $L = \frac{p}{2}r^2\dot{\phi}$. The constant factor $p/2$ can be absorbed into the constant L , however, the effective potential retains the same form given in (55).

Note that for $0 \leq p \leq 2$ the effective potential for the black hole with electric charge has the reversed sign with respect to the corresponding potential in (48).

If one uses the solution with the magnetic ansatz, the null geodesics of the effective geometry (52) satisfy in the equatorial plane $\theta = \frac{\pi}{2}$ a slightly modified equation (as opposed to the electric case):

$$-f(r)\dot{t}^2 + \frac{\dot{r}^2}{f(r)} + (2q-1)r^2\dot{\varphi}^2 = 0, \quad (56)$$

which, however, reduces to (54) once one takes into account (28). Therefore, in the magnetic case one has the same effective potential (55).

The effects of this effective potential are strange! There should be a stable circular orbit for photons, while photons with low energies fall directly into the black hole, those with high energies are scattered back to infinity and do not enter the black hole. However, the interpretation of (55) as an effective potential is not the correct one once one notices the signature of the effective geometry on which photons propagate as in (56). Basically, the nonlinear photons will see the radial coordinate r in the static patch as a timelike coordinate. Their trajectories could be integrated directly, however, we will leave this subject for further work [47].

5 The Klein-Gordon equation and the eikonal approximation

For an uncharged massive boson of mass μ , the Klein-Gordon equation can be written in the form [48], [49], [50]:

$$\frac{1}{r^2}\frac{\partial}{\partial r}\left[r^2f(r)\frac{\partial\Phi}{\partial r}\right] + \frac{1}{r^2\sin\theta}\frac{\partial}{\partial\theta}\left[\sin\theta\frac{\partial\Phi}{\partial\theta}\right] + \frac{1}{r^2\sin^2\theta}\frac{\partial^2\Phi}{\partial\varphi^2} - \frac{1}{f(r)}\frac{\partial^2\Phi}{\partial t^2} - \mu^2\Phi = 0. \quad (57)$$

With the variables separation using the ansatz:

$$\Phi = F(r)Y_\ell^m(\theta, \varphi)e^{-i\omega t}, \quad (58)$$

where Y_ℓ^m are the spherical functions, one obtains to the following differential equation for the radial function

$$\frac{1}{r^2}\frac{d}{dr}\left[r^2f(r)\frac{dF}{dr}\right] + \left[\frac{\omega^2}{f(r)} - \frac{\ell(\ell+1)}{r^2} - \mu^2\right]F = 0. \quad (59)$$

This can be analytically solved only for very few values of the parameter p . For example, for $p = 0$, the solutions are given by the Confluent Heun functions [51] as

$$F(r) = e^{-\alpha x/2}(r - r_h)^{\beta/2} \text{HeunC}[\alpha, \pm\beta, \gamma, \delta, \eta, x], \quad (60)$$

of variable

$$x = 1 - \frac{r}{r_b},$$

with r_b given in (6) and parameters

$$\begin{aligned} \alpha &= -\frac{4iM}{a^2} \sqrt{\omega^2 - a\mu^2}, \quad \beta = -\frac{4iM\omega}{a^2}, \quad \gamma = 0, \quad \delta = \frac{4M^2(2\omega^2 - a\mu^2)}{a^4}, \\ \eta &= -\delta - \frac{l(l+1)}{a}, \end{aligned} \quad (61)$$

with $a = 1 - k$.

In order to have a polynomial form of the confluent Heun functions, one has to impose the necessary condition [51]

$$\frac{\delta}{\alpha} = - \left[n + 1 + \frac{\beta + \gamma}{2} \right]. \quad (62)$$

In the particular case $\mu = 0$, this leads to the imaginary energy spectrum

$$\omega = -i \frac{(n+1)a^2}{4M}, \quad (63)$$

from which, for $k = 0$, we recover the equally spaced energy spectrum of the Schwarzschild black hole:

$$\omega = -i \frac{(n+1)}{4M}.$$

As expected, the solution of the Klein–Gordon equation and the energy spectrum are affected by the parameter $a = 1 - k$ which codifies the presence of the cloud of strings.

In the physically important case $p = 1$, the black hole in the power-Maxwell electrodynamics is described by the metric function (7) which can be written as

$$f(r) = 1 - \frac{2M}{r} - kr = -\frac{k}{r}(r - r_+)(r - r_-), \quad (64)$$

where r_{\pm} are defined in (8). The corresponding radial equation can be analytically solved only in the massless case. The solutions are given by the general Heun functions as [51]

$$F(r) = C_{1,2} (r - r_+)^{\frac{i\omega r_+}{k(r_+ - r_-)}} (r - r_-)^{\frac{\pm i\omega r_-}{k(r_+ - r_-)}} \text{HeunG} [a, q, \alpha_{1,2}, \beta, \gamma, \delta, x], \quad (65)$$

with the variable

$$x = 1 - \frac{r}{r_-}$$

and the parameters

$$a = \frac{r_- - r_+}{r_-}, \quad \alpha_1 = 1 - \frac{i\omega}{k} \frac{(r_+ + r_-)}{(r_+ - r_-)} - \frac{\sqrt{k^2 - \omega^2}}{k}, \quad \alpha_2 = 1 - \frac{i\omega}{k} - \frac{\sqrt{k^2 - \omega^2}}{k}.$$

In order to have a polynomial form of the general Heun functions, one has to impose that the α parameter satisfies the necessary condition $\alpha = -n$, with n a positive integer [51]. For $\alpha_1 = -n$, this condition leads to the following imaginary energy spectrum depending on M and k ,

$$\omega_n = -\frac{i(n+1)}{8M}\sqrt{1-8kM} \left[1 \pm \sqrt{1 - \frac{8kMn(n+2)}{(n+1)^2}} \right]. \quad (66)$$

On the other hand, for the second solution in (65), the condition $\alpha_2 = -n$ leads to a non-trivial energy spectrum depending only on k , i.e.

$$\omega_n = -\frac{ik}{2} \left[\frac{n(n+2)}{n+1} \right].$$

5.1 The eikonal approximation

Finally, let us mention that a relation between the results obtained in the sections 4 and 5 can be established once we make the transition from the Klein–Gordon equation to the classical limit of the particles moving along timelike or null geodesics. In the eikonal approximation, the effective potential (48) should be the same with the one coming from the Klein–Gordon equation [20].

To prove this, we have to perform a change of function in the equation (59),

$$F(r) = \frac{S(r)}{r},$$

which becomes

$$\frac{d}{dr} \left[f(r) \frac{dS}{dr} \right] + \left[\frac{\omega^2}{f(r)} - \frac{\ell(\ell+1)}{r^2} - \mu^2 - \frac{f'(r)}{r} \right] S = 0 \quad (67)$$

Using the tortoise coordinate

$$\frac{dr_*}{dr} = \frac{1}{f(r)},$$

the equation (67), in the massless case, turns into the Schrodinger-like expression

$$\frac{d^2S}{dr_*^2} + \left\{ \omega^2 - f(r) \frac{l(l+1)}{r^2} - \frac{1}{2r} \frac{d}{dr} (f(r)^2) \right\} S = 0 \quad (68)$$

In the eikonal approximation, meaning very large values of l , the above equation has the form

$$\frac{d^2S}{dr_*^2} + \left[\omega^2 - f(r) \frac{l^2}{r^2} \right] S = 0.$$

One may notice the same potential as the one given in (48), while r_0 from (50) which extremizes this potential is known as the radius of the ‘photon sphere’.

5.2 The Hawking temperature for $p = 1$

Classically speaking, a particle inside the event horizon is trapped within and cannot escape. However, in Quantum Mechanics, a particle can tunnel the horizon barrier and escape to an outgoing geodesic. The Hawking radiation of massless particles can be seen as a tunneling process through the horizon and the amplitude for black hole to emit particles is related to the amplitude for it to absorb them.

For the metric function (7), the solution to the Klein–Gordon equation is given in terms of the radial function (65). At the black hole’s horizon $r \rightarrow r_-$, where one of the four singularities of the Heun general function is located and $HeunG(0) \approx 1$, the outgoing wave solution has the expression

$$\Phi(r, t) \approx e^{-i\omega t} (r - r_-)^{\frac{i\omega r_-}{k(r_+ - r_-)}} \quad (69)$$

and the relative scattering probability is given by the relation [52]

$$\Gamma = \left| \frac{\Phi_{out}(r > r_-)}{\Phi_{out}(r < r_-)} \right|^2 = \exp \left[-\frac{4\pi\omega r_-}{k(r_+ - r_-)} \right].$$

This leads to the mean number of emitted particles

$$N = \frac{\Gamma}{1 - \Gamma} = \frac{1}{e^{\frac{\omega}{T}} - 1},$$

pointing out the Hawking temperature on the black hole horizon,

$$T_b = \frac{k(r_+ - r_-)}{4\pi r_-} = \frac{1 - 2kr_-}{4\pi r_-} = \frac{k\sqrt{1 - 8kM}}{2\pi(1 - \sqrt{1 - 8kM})}. \quad (70)$$

This result agrees with the one derived in [53], using a different approach.

6 Thermodynamic properties of the Kiselev black hole in power-Maxwell electrodynamics

In this section we will initiate the study of the thermodynamics of the Kiselev black holes in the power-Maxwell nonlinear electrodynamics using the electric ansatz from section 3. The magnetic case is completely similar. As we have seen in section 3.3, this geometry can have at most two horizons, one black hole horizon, located at r_b and one outer, cosmological-type horizon located at $r_c > r_b$. Depending on the values of the parameters, if one increases the mass M then r_b increases while r_c decreases, *i. e.* the two horizons get closer and closer and they will coincide in this coordinate system if the mass reaches the maximum value (33). If

one increases the mass parameter beyond this maximum value the geometry will have no horizon, while it will generically have a naked curvature singularity in origin.

To compute the black hole temperature we will make use of the definition of the surface gravity:

$$k_b^2 = -\frac{1}{2}\nabla_\mu\xi_\nu\nabla^\mu\xi^\nu, \quad (71)$$

where ξ^μ is a Killing vector field which is null on the black hole horizon. Since our metric is static one picks $\xi^\mu = \frac{\partial}{\partial t}$ such that the surface gravity becomes $k_b = \frac{f'(r_b)}{2}$ and the black hole temperature becomes:

$$T_b = \frac{k_b}{2\pi} = \frac{f'(r_b)}{4\pi} = \frac{p - 2^{\frac{2-p}{4}}Q_e^{\frac{2-p}{2}}r_b^p}{4\pi pr_b}, \quad (72)$$

where r_b is the radius of the event horizon. For very small values of the black hole horizon radius r_b one can see from (72) that $T_b \rightarrow \frac{1}{4\pi r_b}$, which is the temperature of a Schwarzschild black hole with horizon radius $r_b = 2M$. Note that r_b can only increase up to the maximum value r_0 in (32) that corresponds to the extremal case when the black hole and the cosmological horizon coincide. In terms of the electric charge Q_e and the parameter p , this maximum value of the black hole horizon can be expressed as:

$$r_0 = Q_e^{\frac{2-p}{2p}} \left(2^{\frac{p-2}{4}}p\right)^{\frac{1}{p}}. \quad (73)$$

This is precisely the value for which the black hole temperature (72) reaches zero, as expected.

One can associate as well a temperature to the cosmological horizon, r_c :

$$T_c = -\frac{k_c}{2\pi} = -\frac{f'(r_c)}{4\pi}. \quad (74)$$

The minus sign appears here in order to account for the fact that $k_c < 0$ on the cosmological horizon.

Note that the entropy of these black holes should satisfy the area-law, which means that the black hole entropy is $S_b = \frac{A_b}{4}$, where A_b is the area of the black hole horizon. One can also associate an entropy with the cosmological horizon $S_c = \frac{A_c}{4}$, where A_c is the area of the cosmological horizon. The situation here is reminiscent of black holes in de Sitter spacetime. Once again one has a black hole horizon surrounded by an outer, cosmological horizon and the two horizons will coincide in the extremal case, described by the so-called Nariai-de Sitter black hole.

Similarly to the black hole in the de Sitter case, an important difficulty is associated with the definition of the quasilocal mass for this class of spacetimes. The problem arises

here because of the absence of a globally-defined timelike Killing vector at spacial infinity. However, there does exist a Killing vector that is timelike inside the static patch of the Kiselev geometry, while it becomes spacelike outside the cosmological horizon and this vector could still be used to define a notion of quasilocal mass. Another problem is related to the fact that for general values of p the spacetime is not asymptotically de Sitter, nor asymptotically flat and there are no counterterms known to render the action and the conserved physical quantities finite.

However, to compute the quasilocal mass one can still make use of the background subtraction method of Brown and York [54], [55]. Unlike the counterterm method in de Sitter case [56], this procedure will produce results that depend on the choice of the reference background. Let us begin by writing the metric induced on equal time surfaces (they are the $r = \text{const.}$ surfaces outside the cosmological horizon) in the form:

$$h_{ab}dx^a dx^b = -f(r)dt^2 + r^2(d\theta^2 + \sin^2\theta d\varphi^2) \equiv -f(r)dt^2 + \sigma_{ij}d\phi^i d\phi^j. \quad (75)$$

If $\xi^\mu = \frac{\partial}{\partial t}$ is the Killing vector generating an isometry on the boundary and if $n_\mu = [\sqrt{-f(r)}, 0, 0, 0]$ is the unit normal on a surface of fixed t then, following [56] we define the conserved charge associated to the Killing vector ξ^μ using the formula:

$$\mathcal{M} = \frac{1}{8\pi} \int_{S^2} d^2\phi \sqrt{\sigma} T_{ab} \xi^a n^b, \quad (76)$$

where we defined [54], [55]:

$$T_{ab} = (K_{ab} - K h_{ab}) - (K_{ab}^0 - K^0 h_{ab}^0). \quad (77)$$

Here K_{ab} is the extrinsic curvature of the metric (75) induced on the boundary, K is its trace, while K_{ab}^0 , K^0 and h_{ab}^0 are the corresponding quantities computed for the reference background. This mass formula is used for a surface of fixed time r outside the cosmological horizon, while in the limit in which this boundary is pushed to future infinity $r \rightarrow \infty$ one obtains a finite result for the conserved quasilocal mass.

In our case we shall pick the reference geometry as the one corresponding to $M = 0$ in (14). A simple computation leads to a remarkable simple formula for the conserved mass:

$$\mathcal{M} = \lim_{r \rightarrow \infty} r \sqrt{-f(r)} [\sqrt{-f^0(r)} - \sqrt{f(r)}], \quad (78)$$

which can be compared to a similar expression derived in [57]. Using now the function (14) while $f^0(r) = 1 - kr^p$, one obtains the quasilocal mass $\mathcal{M} = M$.

To express the mass $\mathcal{M} = M$ in terms of the extensive parameters S_b and Q_e we shall use the relation $f(r_b) = 0$. One obtains:

$$\mathcal{M} = \frac{r_b}{2p(p+1)} \left(p(p+1) - 2^{\frac{2-p}{4}} Q_e^{\frac{2-p}{2}} r_b^p \right). \quad (79)$$

One can now check that $T_b = \left(\frac{\partial \mathcal{M}}{\partial S_b}\right)_{Q_e}$ is indeed the Hawking temperature (72), where $S_b = \pi r_b^2$ is the black hole entropy.

If one defines the electric potential:

$$\Phi_b^e = \left(\frac{\partial \mathcal{M}}{\partial Q_e}\right)_{S_b} = \frac{p-2}{2p} \frac{Q_e^{\frac{2-p}{2}} r_b^{p+1}}{2^{\frac{2+p}{4}}(p+1)}, \quad (80)$$

then it is easy to verify that the first law of thermodynamics is satisfied:

$$d\mathcal{M} = T_b dS_b + \Phi_b^e dQ_e, \quad (81)$$

as well as a Smarr like relation of the form:

$$\mathcal{M} = 2T_b S_b + \frac{2p}{p-2} \Phi_e Q_e. \quad (82)$$

This is precisely the same Smarr relation found in [28], as expected. Note that there are similar relations corresponding to the cosmological horizon r_c :

$$d\mathcal{M} = -T_c dS_c + \Phi_c^e dQ_e, \quad (83)$$

where

$$\Phi_c^e = \left(\frac{\partial \mathcal{M}}{\partial Q_e}\right)_{S_c} = \frac{p-2}{2p} \frac{Q_e^{\frac{2-p}{2}} r_c^{p+1}}{2^{\frac{2+p}{4}}(p+1)}, \quad (84)$$

while

$$\mathcal{M} = -2T_c S_c + \frac{2p}{p-2} \Phi_c^e Q_e. \quad (85)$$

We are now ready to investigate the thermal stability using the canonical ensemble method⁴. We shall compute the black hole heat capacity while keeping the black hole charge Q_e as constant. The heat capacity becomes:

$$C_{Q_e} = T_b \left(\frac{\partial S_b}{\partial T_b}\right)_{Q_e} = \frac{T_b}{M_{SS}}, \quad (86)$$

where we defined $M_{SS} = \left(\frac{\partial^2 \mathcal{M}}{\partial S_b^2}\right)_{Q_e}$. Positivity of C_{Q_e} or M_{SS} would be sufficient to ensure the local stability of our black holes in the power-Maxwell electrodynamics. In our case T_b

⁴There are also stability conditions that can be checked at the level of the nonlinear electrodynamics Lagrangian [58].

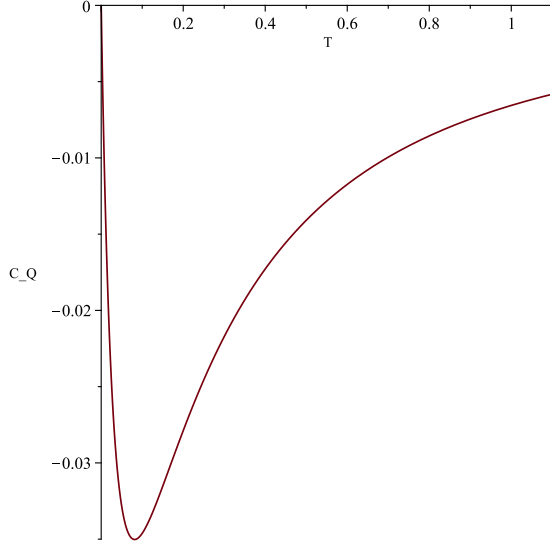


Figure 4: The heat capacity, C_{Q_e} versus the temperature T_b for $Q_e = 0.5$ and $p = \frac{2}{5}$. One can notice the presence of a Schottky peak.

is positive and it reaches the zero value for $r_b = r_0$ from (73). Therefore, one should turn our attention to the quantity:

$$M_{SS} = -\frac{p + (p-1)2^{\frac{2-p}{4}}Q_e^{\frac{2-p}{2}}r_b^p}{8\pi^2 pr_b^3}. \quad (87)$$

Since $p \in [0, 2]$ there might be values for r_b for which $M_{SS} = 0$ if $0 \leq p \leq 1$, which generically will lead to divergences in the heat capacity C_{Q_e} , signaling type 2 phase transitions. However, if one recalls the expression of r_0 from (73) then one can express the quantity M_{SS} as:

$$M_{SS} = -\frac{1 - (1-p)\left(\frac{r_b}{r_0}\right)^p}{8\pi^2 r_b^3}. \quad (88)$$

It is now clear that if $0 \leq p \leq 1$ then M_{SS} can have a real root $r_b = r_0(1-p)^{-\frac{1}{p}}$, however this value is always greater than the maximum value r_0 that can be reached by the black hole horizon. In conclusion, in the interval $0 \leq r_b \leq r_0$ the heat capacity is always negative and the black hole system in the power-Maxwell electrodynamics is unstable for $p \leq 2$. The point $r_b = r_0$ is a bound point of the heat capacity, since for this value one has $C_{Q_e} = T_b = 0$. However, at this location the heat capacity does not change sign and there are no type 1 phase transitions since there are no physical values of the black hole horizon radius r_b beyond the limit r_0 given in (73) for which the heat capacity C_{Q_e} could reach positive values.

The black hole temperature T_b varies from 0 to ∞ . The value $T_b \rightarrow \infty$ is attained in the limit $r_b \rightarrow 0$. From (86) and (88) it should be clear that in this limit $C_{Q_e} \rightarrow 0$. As shown

in Figure 4 this signals the presence of a Schottky peak [44], [45], [46] in the dependence of temperature of the heat capacity (86).

With hindsight, the presence of a Schottky peak was to be expected in our case. They usually appear in multi-horizon spacetimes (although they have been noticed in the anti-de Sitter case as well [46]), such as black holes in de Sitter geometry, for which there is a cap in the energy of the system. In this case the dependence of the heat capacity as a function of temperature could give us important clues regarding the underlying degrees of freedom for such systems. One should note that, similar to the Schwarzschild - de Sitter case, the existence of the Schottky peaks is directly related to the existence of a cosmological horizon [44].

Furthermore, the existence of the Schottky peak hints to the intriguing possibility of using the black hole in the power-Maxwell electrodynamics to function as a continuous heat engine [45]. More precisely, combining (81) with (83) one obtains:

$$2d\mathcal{M} = T_b dS_b - T_c dS_c + (\Phi_b^e + \Phi_c^e) dQ_e. \quad (89)$$

The continuous heat engine mode of operation will leave the black hole energy fixed $d\mathcal{M} = 0$ such that:

$$T_b dS_b = T_c dS_c - (\Phi_b^e + \Phi_c^e) dQ_e. \quad (90)$$

Consider now the case with $dQ_e < 0$, with an increase of the black hole entropy $dS_b > 0$ such that there is a positive heat inflow $Q_H = T_b dS_b > 0$, with $Q_C = T_c dS_c$ the heat flow away from the black hole. Then $W = -(\Phi_b^e + \Phi_c^e) dQ_e > 0$ is the positive work done in this cycle.

7 Conclusions

In recent years, Kiselev's solution has received increased interest in connection to the properties of the anisotropic fluid sourcing this geometry, properties that mimic a dark energy source. In the present work we found a physical source for the Kiselev geometry within the context of nonlinear electrodynamics theories. More specifically, in section 3 we showed that the Kiselev geometry becomes an exact solution of the Einstein equations coupled to power-Maxwell electrodynamics, using either an electric or a magnetic ansatz. We also checked the energy conditions showing that the weak energy condition (WEC) and the dominant energy condition (DEC) are both satisfied, while the strong energy condition (SEC) is violated in both cases.

In section 4 we studied the trajectories of particles that follow the timelike and the null geodesics of this geometry. However, in the nonlinear electrodynamics theories it turns out

that photons will not follow the null geodesics of the background Kiselev geometry, instead they move along the null geodesics of an effective geometry, defined in (52). As it appears, the nonlinear photons will see the radial coordinate r in the static patch as a timelike coordinate, while the time coordinate t becomes spacelike (just as these coordinates change their roles when crossing a horizon). Their trajectories could be integrated directly, however, we will leave this subject for further work [47].

In section 5 we have solved the Klein-Gordon equation for massless particles evolving in the Kiselev geometry. Besides the $p = 0$ case where the calculations are significantly simpler, we have focused on the case corresponding to $p = 1$. This is important not only because one can find an analytical solution to the Klein-Gordon equation, but also because this particular value of p is close to the limit imposed in confrontation with observations [17]. In both cases under consideration, the imaginary energy spectrum can be derived by imposing that the Heun functions get a polynomial form. One may notice that the frequencies of the scalar field in the Schwarzschild black hole in the power-Maxwell electrodynamics, given by (63) and (66), are influenced by the nonlinear electromagnetic fields, their magnitude being lower compared to the ones corresponding to the Schwarzschild black hole [59]. Such investigations are very important since perturbations of a black hole can be studied not only by adding perturbation terms in the spacetime metric, but also by considering fields on the corresponding manifold. The quasi-normal modes dominate the gravitational-wave response if the spectrum of the external source that perturbed the black hole is close to the fundamental frequencies of the black hole. The quasi-normal frequencies are depending only on the black hole's parameters and that is why they carry the characteristic information of the black hole [60].

In section 6 we investigated the thermodynamics of the Kiselev solution in the power-Maxwell geometry for the electric case. We computed the mass using the Brown-York subtraction method and showed that the first law of thermodynamics and a modified Smarr relation are both satisfied. The black hole in this case has negative heat capacity and it is therefore unstable, while it exhibits a Schottky peak in the dependence of the heat capacity as a function of temperature. Similarly to the de Sitter case, the presence of the Schottky peak hints to the possibility of using this black hole as a continuous heat engine.

As avenues for further work, it might be interesting to investigate the effects of nonlinear power-Maxwell fields in constructing interior fluid solutions, which describe compact objects in General Relativity. Such solutions can be generated easily for the usual Maxwell electrodynamics [61], [62] and it might be fruitful to further investigate this matter. Work on these issues is in progress and it will be reported elsewhere.

References

- [1] A. G. Riess *et al.*, Astron. J. **116**, 1009 (1998).
- [2] S. Perlmutter *et al.*, Astrophys. J. **517**, 565 (1999).
- [3] D. N. Spergel *et al.* [WMAP Collaboration], Astrophys. J. Suppl. **148**, 175 (2003).
- [4] P. A. R. Ade *et al.* [Planck Collaboration], arXiv:1303.5076 [astro-ph.CO].
- [5] D. J. Eisenstein *et al.* [SDSS Collaboration], Astrophys. J. **633**, 560 (2005).
- [6] T. Padmanabhan, Phys. Rept. **380**, 235-320 (2003) doi:10.1016/S0370-1573(03)00120-0 [arXiv:hep-th/0212290 [hep-th]].
- [7] S. Capozziello, V. F. Cardone, E. Piedipalumbo and C. Rubano, Class. Quant. Grav. **23**, 1205-1216 (2006) doi:10.1088/0264-9381/23/4/009 [arXiv:astro-ph/0507438 [astro-ph]].
- [8] A. Vikman, Phys. Rev. D **71**, 023515 (2005) doi:10.1103/PhysRevD.71.023515 [arXiv:astro-ph/0407107 [astro-ph]].
- [9] S. Tsujikawa, Class. Quant. Grav. **30**, 214003 (2013) doi:10.1088/0264-9381/30/21/214003 [arXiv:1304.1961 [gr-qc]].
- [10] S. Capozziello, S. Nojiri and S. D. Odintsov, Phys. Lett. B **634**, 93-100 (2006) doi:10.1016/j.physletb.2006.01.065 [arXiv:hep-th/0512118 [hep-th]].
- [11] C. Dariescu, Int. J. Mod. Phys. D **13**, 641-657 (2004) doi:10.1142/S0218271804003676 [arXiv:gr-qc/0302019 [gr-qc]]. Dariescu, C., Dariescu M. Found Phys 21, 1323–1327 (1991). <https://doi.org/10.1007/BF00732834>;
M. A. Dariescu and C. Dariescu 2007 J. Phys.: Condens. Matter 19 256203;
O. Buhucianu et al. International Journal of Theoretical Physics 51 (2012): 526-535.
- [12] F. S. Guzman, T. Matos, D. Nunez and E. Ramirez, Rev. Mex. Fis. **49**, 203-206 (2003) [arXiv:astro-ph/0003105 [astro-ph]].
- [13] V. V. Kiselev, Class. Quant. Grav. **20**, 1187-1198 (2003) doi:10.1088/0264-9381/20/6/310 [arXiv:gr-qc/0210040 [gr-qc]].
- [14] M. Visser, Class. Quant. Grav. **37**, no.4, 045001 (2020) doi:10.1088/1361-6382/ab60b8 [arXiv:1908.11058 [gr-qc]].

[15] P. Boonserm, T. Ngampitipan, A. Simpson and M. Visser, Phys. Rev. D **101**, no.2, 024022 (2020) doi:10.1103/PhysRevD.101.024022 [arXiv:1910.08008 [gr-qc]].

[16] Mannheim, P. D. & Kazanas, D. 1989, Astrophysical Journal, 342, 635. doi:10.1086/167623

[17] D. Gregoris, Y. C. Ong and B. Wang, Eur. Phys. J. C **81**, no.8, 684 (2021) doi:10.1140/epjc/s10052-021-09464-3 [arXiv:2106.05205 [gr-qc]].

[18] S. Panpanich and P. Burikham, Phys. Rev. D **98**, no.6, 064008 (2018) doi:10.1103/PhysRevD.98.064008 [arXiv:1806.06271 [gr-qc]].

[19] Toledo, J. M. & Bezerra, V. B. 2020, General Relativity and Gravitation, 52, 34. doi:10.1007/s10714-020-02683-1

[20] M. A. Dariescu and C. Dariescu, Eur. Phys. J. Plus **137**, no.2, 238 (2022) doi:10.1140/epjp/s13360-022-02464-6

[21] Born, M. Nature 132, 282 (1933). <https://doi.org/10.1038/132282a0>, Born, M., Infeld, L. Nature 132, 1004 (1933). <https://doi.org/10.1038/1321004b0>

[22] Heisenberg, W. & Euler, H. 2006, physics/0605038

[23] N. Breton and R. Garcia-Salcedo, [arXiv:hep-th/0702008 [hep-th]].

[24] A. Bokulić, T. Jurić and I. Smolić, Phys. Rev. D **103**, no.12, 124059 (2021) doi:10.1103/PhysRevD.103.124059 [arXiv:2102.06213 [gr-qc]].

[25] D. P. Sorokin, [arXiv:2112.12118 [hep-th]].

[26] G. W. Gibbons and C. A. R. Herdeiro, Class. Quant. Grav. **18**, 1677-1690 (2001) doi:10.1088/0264-9381/18/9/305 [arXiv:hep-th/0101229 [hep-th]].

[27] M. Hassaine and C. Martinez, Class. Quant. Grav. **25**, 195023 (2008) doi:10.1088/0264-9381/25/19/195023 [arXiv:0803.2946 [hep-th]].

[28] H. A. Gonzalez, M. Hassaine and C. Martinez, Phys. Rev. D **80**, 104008 (2009) doi:10.1103/PhysRevD.80.104008 [arXiv:0909.1365 [hep-th]].

[29] M. Hassaine and C. Martinez, Phys. Rev. D **75**, 027502 (2007) doi:10.1103/PhysRevD.75.027502 [arXiv:hep-th/0701058 [hep-th]].

[30] B. Eslam Panah, EPL **134**, 20005 (2021) doi:10.1209/0295-5075/134/20005 [arXiv:2103.08343 [physics.class-ph]].

[31] B. E. Panah, K. Jafarzade and A. Rincon, [arXiv:2201.13211 [physics.gen-ph]].

[32] S. H. Hendi, B. E. Panah and S. Panahiyan, Fortsch. Phys. **66**, no.3, 1800005 (2018) doi:10.1002/prop.201800005 [arXiv:1708.02239 [hep-th]].

[33] S. H. Hendi, B. Eslam Panah, S. Panahiyan and A. Sheykhi, Phys. Lett. B **767**, 214-225 (2017) doi:10.1016/j.physletb.2017.01.066 [arXiv:1703.03403 [gr-qc]].

[34] S. H. Hendi, B. Eslam Panah, S. Panahiyan and M. S. Talezadeh, Eur. Phys. J. C **77**, no.2, 133 (2017) doi:10.1140/epjc/s10052-017-4693-0 [arXiv:1612.00721 [hep-th]].

[35] S. H. Hendi and B. E. Panah, Phys. Lett. B **684**, 77-84 (2010) doi:10.1016/j.physletb.2010.01.026 [arXiv:1008.0102 [hep-th]].

[36] M. E. Rodrigues, M. V. de S. Silva and H. A. Vieira, Phys. Rev. D **105**, no.8, 084043 (2022) doi:10.1103/PhysRevD.105.084043 [arXiv:2203.04965 [gr-qc]].

[37] M. Novello, V. A. De Lorenci, J. M. Salim and R. Klippert, Phys. Rev. D **61**, 045001 (2000) doi:10.1103/PhysRevD.61.045001 [arXiv:gr-qc/9911085 [gr-qc]].

[38] A. S. Habibina and H. S. Ramadhan, Phys. Rev. D **101**, no.12, 124036 (2020) doi:10.1103/PhysRevD.101.124036 [arXiv:2007.03211 [gr-qc]].

[39] S. Fernando, Gen. Rel. Grav. **44**, 1857-1879 (2012) doi:10.1007/s10714-012-1368-x [arXiv:1202.1502 [gr-qc]].

[40] S. Fernando, S. Meadows and K. Reis, Int. J. Theor. Phys. **54** (2015) no.10, 3634-3653 doi:10.1007/s10773-015-2601-7 [arXiv:1411.3192 [gr-qc]].

[41] R. Uniyal, N. Chandrachani Devi, H. Nandan and K. D. Purohit, Gen. Rel. Grav. **47**, no.2, 16 (2015) doi:10.1007/s10714-015-1857-9 [arXiv:1406.3931 [gr-qc]].

[42] M. A. Dariescu and C. Dariescu, Eur. Phys. J. Plus **136**, no.4, 375 (2021) doi:10.1140/epjp/s13360-021-01375-2

[43] Al-Badawi, A., Kanzi, S., & Sakallı, I. 2020, European Physical Journal Plus, 135, 219. doi:10.1140/epjp/s13360-020-00245-7

[44] J. Dinsmore, P. Draper, D. Kastor, Y. Qiu and J. Traschen, Class. Quant. Grav. **37** (2020) no.5, 054001 doi:10.1088/1361-6382/ab638f [arXiv:1907.00248 [hep-th]].

- [45] C. V. Johnson, [arXiv:1907.05883 [hep-th]].
- [46] C. V. Johnson, *Class. Quant. Grav.* **37** (2020) no.5, 054003 doi:10.1088/1361-6382/ab685a [arXiv:1905.00539 [hep-th]].
- [47] C. Stelea, M. A. Dariescu, C. Dariescu (work in progress)
- [48] M. A. Dariescu, C. Dariescu and C. Stelea, *Mod. Phys. Lett. A* **35**, no.07, 2050036 (2019) doi:10.1142/S0217732320500364 [arXiv:1903.03552 [hep-th]].
- [49] C. Dariescu, M. A. Dariescu and C. Stelea, *Gen. Rel. Grav.* **49**, no.12, 153 (2017) doi:10.1007/s10714-017-2314-8
- [50] M. A. Dariescu, C. Dariescu and C. Stelea, *Gen. Rel. Grav.* **50**, no.10, 126 (2018) doi:10.1007/s10714-018-2449-2
- [51] A. Ronveaux, *Heun's differential equations*, Oxford Science Publications (The Clarendon Press Oxford University Press,1995).
S. Yu. Slavianov and W. Lay, *Special Functions: A Unified Theory Based on Singularities*, Oxford University Press (2000).
- [52] H. S. Vieira, V. B. Bezerra and G. V. Silva, *Annals Phys.* **362**, 576-592 (2015) doi:10.1016/j.aop.2015.08.027 [arXiv:1501.00462 [gr-qc]].
- [53] Eslamzadeh, S. & Nozari, K. 2020, *Nuclear Physics B*, 959, 115136. doi:10.1016/j.nuclphysb.2020.115136
- [54] J. D. Brown and J. W. York, Jr., *Phys. Rev. D* **47** (1993), 1407-1419 doi:10.1103/PhysRevD.47.1407 [arXiv:gr-qc/9209012 [gr-qc]].
- [55] J. D. Brown, J. Creighton and R. B. Mann, *Phys. Rev. D* **50** (1994), 6394-6403 doi:10.1103/PhysRevD.50.6394 [arXiv:gr-qc/9405007 [gr-qc]].
- [56] V. Balasubramanian, J. de Boer and D. Minic, *Phys. Rev. D* **65** (2002), 123508 doi:10.1103/PhysRevD.65.123508 [arXiv:hep-th/0110108 [hep-th]].
- [57] K. C. K. Chan, J. H. Horne and R. B. Mann, *Nucl. Phys. B* **447** (1995), 441-464 doi:10.1016/0550-3213(95)00205-7 [arXiv:gr-qc/9502042 [gr-qc]].
- [58] C. Moreno and O. Sarbach, *Phys. Rev. D* **67** (2003), 024028 doi:10.1103/PhysRevD.67.024028 [arXiv:gr-qc/0208090 [gr-qc]].

[59] N. Varghese and V. C. Kuriakose, *Gen. Rel. Grav.* **41**, 1249-1257 (2009) doi:10.1007/s10714-008-0702-9 [arXiv:0802.1397 [gr-qc]].

[60] K. D. Kokkotas and B. G. Schmidt, *Living Rev. Rel.* **2**, 2 (1999) doi:10.12942/lrr-1999-2 [arXiv:gr-qc/9909058 [gr-qc]].

[61] C. Stelea, M. A. Dariescu and C. Dariescu, *Phys. Rev. D* **97** (2018) no.10, 104059 doi:10.1103/PhysRevD.97.104059 [arXiv:1804.08075 [gr-qc]].

[62] C. Stelea, M. A. Dariescu and C. Dariescu, [arXiv:1810.02235 [gr-qc]].